



# Upgrade Your NMR Console for Peak Performance

*A PROUD MANUFACTURER OF NMR SYSTEMS SINCE 1956*



## NMR Upgrade

## RESEARCH ARTICLE

WILEY

## Micellar and solubilizing properties of rhamnolipids

Victor P. Arkhipov<sup>1</sup>  | Ruslan V. Arkhipov<sup>2</sup> | Ekaterina V. Petrova<sup>3</sup>  |  
Andrei Filippov<sup>4</sup> <sup>1</sup>Department of Physics, Kazan National Research Technological University, Kazan, 420015, Russian Federation<sup>2</sup>Institute of Physics, Kazan Federal University, Kazan, 420008, Russian Federation<sup>3</sup>Department of Analytical Chemistry, Kazan National Research Technological University, Kazan, 420015, Russian Federation<sup>4</sup>Chemistry of Interfaces, Luleå University of Technology, Luleå, SE-97187, Sweden

## Correspondence

Andrei Filippov, Chemistry of Interfaces, Luleå University of Technology, Luleå, Sweden.

Email: [andrei.filippov@ltu.se](mailto:andrei.filippov@ltu.se)

## Funding information

Ministry of Science and Higher education of the Russian Federation, Grant/Award Number: 075-15-2021-699; Program Priority-2030 for Kazan Federal University

## Abstract

We studied the micellar and solubilizing properties of aqueous solutions of unfractionated rhamnolipids produced by *Pseudomonas aeruginosa*. We used nuclear magnetic resonance (NMR) diffusometry, dynamic light scattering, and conductometry to measure the critical micelle concentration (CMC) of rhamnolipid solutions and determined the effective hydrodynamic radii of rhamnolipid monomers and micelles. Based on selective measurements of the self-diffusion coefficients of molecules, performed by NMR diffusometry, the solubilizing properties of rhamnolipids were studied depending on their concentration in solution; aromatic hydrocarbons, benzene, toluene, ethylbenzene, and para-xylene were taken as solubilizates. On the basis of the measurement results, we estimated the distribution coefficient of the solubilize between the micellar (solubilized) and free (in the aqueous phase) states and the solubilizing capacity of rhamnolipid micelles.

## KEYWORDS

aromatic hydrocarbons, CMC, dynamic light scattering, NMR, rhamnolipids, self-diffusion coefficients, solubilization

## 1 | INTRODUCTION

Rhamnose lipids or rhamnolipids (RLs) are biological surfactants<sup>[1–4]</sup> of the glycolipid class, produced by *Pseudomonas aeruginosa*. RLs have been studied extensively because of their unique physicochemical and biological properties.<sup>[5–7]</sup> RLs are used in environmental remediation,<sup>[8,9]</sup> bioremediation and soil washing,<sup>[10,11]</sup> biodegradation of hydrophobic organic compounds,<sup>[12]</sup> food production,<sup>[13]</sup> cosmetics, and pharmaceuticals.<sup>[14–16]</sup> The ability of RLs to solubilize and enhance the degradation of organic compounds is exploited in soil reclamation after oil and oil product spills<sup>[17,18]</sup> and for remediation of soils contaminated

with heavy metals.<sup>[10,19–21]</sup> Compared with synthetic surfactants, RLs have significantly lower toxicity and high biodegradability.<sup>[22]</sup>

RLs contain a hydrophilic head of one or two rhamnose groups and a hydrophobic tail of one or two 3-hydroxy fatty acids chains (Figure 1). RLs are non-ionic surfactants with high surface activity, emulsifying ability, low surface tension, and low critical micelle concentrations (0.01/0.2 g/L).<sup>[5,6,17,23–26]</sup> At concentrations above the critical micelle concentration (CMC), RLs in aqueous solutions form micelles, vesicles, or lamellae,<sup>[24,25,27–29]</sup> depending on their concentration, pH,<sup>[30]</sup> and the presence of electrolytes<sup>[31–33]</sup> and organic substances.<sup>[34]</sup> RL micelles are able to solubilize lipophilic organic

This is an open access article under the terms of the [Creative Commons Attribution-NonCommercial-NoDerivs](https://creativecommons.org/licenses/by-nc-nd/4.0/) License, which permits use and distribution in any medium, provided the original work is properly cited, the use is non-commercial and no modifications or adaptations are made.

© 2023 The Authors. *Magnetic Resonance in Chemistry* published by John Wiley & Sons Ltd.

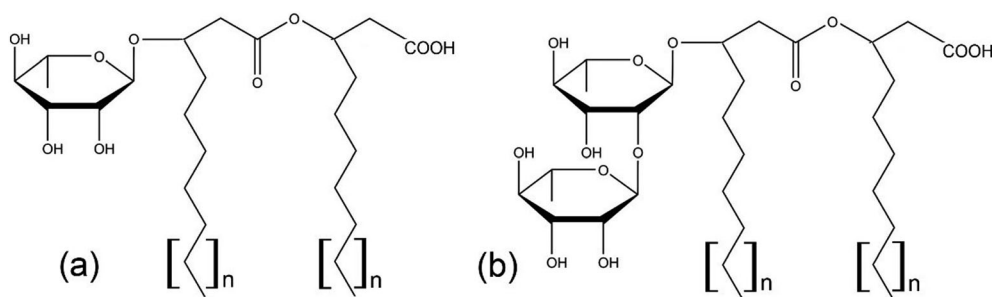


FIGURE 1 Molecular structure of (a) mono-rhamnolipid and (b) di-rhamnolipid.

compounds (aliphatic, aromatic hydrocarbons, polycyclic aromatic hydrocarbons).<sup>[35–40]</sup> Foam flotation<sup>[41]</sup> and micellar ultrafiltration<sup>[42]</sup> methods use RLs to extract inorganic pollutants Cd and Cr<sup>[43–45]</sup> from aqueous media, including industrial effluents.

The effectiveness of RLs in the processes of soil remediation and wastewater treatment is explained by their high solubilizing ability and their ability to transfer organic compounds into bacterial cells, contributing to their further biodegradation. Note that binding of hydrophobic organic compounds by RLs is also observed in the pre-micellar concentration range.<sup>[31,46,47]</sup>

A well-known source of soil, air, and water pollution are products of decomposition and refining of oil. These volatile aromatic hydrocarbons (benzene, toluene, ethylbenzene, and xylene isomers [BTEX])<sup>[48]</sup> and polycyclic aromatic hydrocarbons (PAHs)<sup>[49]</sup> have pronounced carcinogenic, mutagenic, and teratogenic effects; therefore, their maximum permissible concentrations in air, water, and soil are strictly regulated.<sup>[50]</sup> The concentration of BTEX and other hazardous organic compounds in the environment is monitored by chromatography, mass spectroscopy combined with microextraction.<sup>[51,52]</sup> Biological decomposition of BTEX compounds,<sup>[12,53,54]</sup> adsorption<sup>[55,56]</sup> using carbon nanotubes as a sorbent,<sup>[57]</sup> photocatalytic decomposition,<sup>[58]</sup> and electrochemical decomposition methods<sup>[59]</sup> are used to clean up and restore contaminated areas.

Nuclear magnetic resonance (NMR) diffusometry<sup>[60–62]</sup> with a pulsed magnetic field gradient and Fourier transform of the spin echo signal<sup>[63–65]</sup> is an effective, non-destructive method for studying multicomponent solutions of liquids, including surfactant solutions.<sup>[66,67]</sup> This method makes it possible to measure the diffusivities of molecules of all components of the solution in one experiment without introducing any changes to the system under study, for example, by using radioactive isotopes in the traced atom method. The possibility of performing NMR on different nuclei,<sup>[68]</sup> using mathematical processing of diffusion decays in the case of overlapping spectral lines,<sup>[69–71]</sup> makes NMR

diffusometry a unique method for studying the dynamic and structural properties of solutions.<sup>[66,72]</sup>

In this work, we used NMR diffusometry, dynamic light scattering, and conductometry to study the micellar and solubilizing properties of RLs in aqueous solutions containing BTEX compounds at concentrations corresponding to limiting solubilities. In mixtures of liquids, in micellar solutions, NMR diffusometry makes it possible to measure the self-diffusion coefficients of molecules of individual components, micelles, and aggregates. This allows, based on the Stokes–Einstein relation<sup>[73]</sup> with certain assumptions and corrections,<sup>[74]</sup> one to draw conclusions about the sizes, shape, and composition of diffusing particles. By comparing the diffusivities of BTEX molecules and of RL micelles, we calculated the solubilization distribution parameters between the aqueous and micellar media and the solubilization capacities of micelles depending on the concentration of RLs in solutions from 0.05 to 200 g/L. NMR diffusometry, dynamic light scattering, and conductometry were used to determine the CMC of RLs in aqueous solutions. All measurements were performed at a temperature of 298 K.

## 2 | MATERIALS AND METHODS

### 2.1 | Materials

RLs were purchased from Merck (Germany). It is a mixture of mono- and di-RLs produced by AGAE Technologies LLC, Corvallis, Oregon, 97333, USA. The content of RLs in the powder was more than 90%. No additional purification and fractionation were performed. All BTEX hydrocarbons (benzene, toluene, ethylbenzene, and para-xylene) were of chemically pure grade.

All solutions for NMR measurements were prepared in deuterated water, D<sub>2</sub>O (Sigma, degree of substitution 99.9%). Solutions of BTEX at the limiting solubility were prepared by adding excess amounts of BTEX to D<sub>2</sub>O, thoroughly mixing and allowing to settle for several days. Using deuterated water made it possible to exclude the

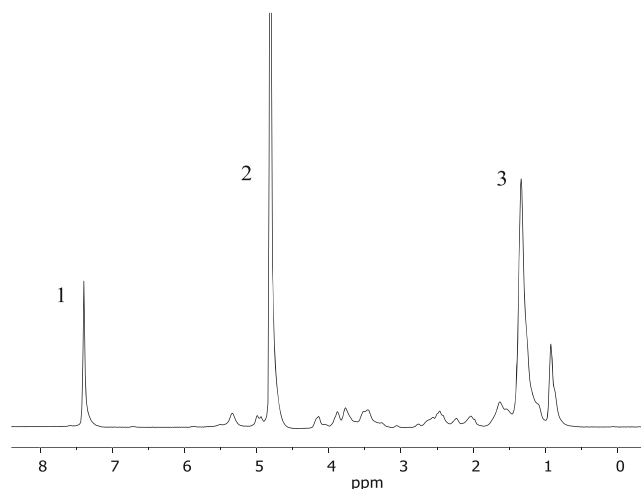


**FIGURE 2**  $^1\text{H}$  nuclear magnetic resonance (NMR) spectrum of rhamnolipids in a saturated solution of benzene: (1) line of aromatic benzene protons, (2) line of residual water protons, (3) line of methylene protons of rhamnolipid.  $T = 298\text{ K}$ .

intense line of water from the  $^1\text{H}$  NMR spectra. Solutions for dynamic light scattering (DLS) and conductometry were prepared in ordinary distilled  $\text{H}_2\text{O}$ .

## 2.2 | NMR spectroscopy and NMR diffusometry

$^1\text{H}$  NMR spectra, spin-lattice relaxation times  $T_1$ , and self-diffusion coefficients of molecules were recorded and measured on a Bruker Avance NMR spectrometer with a resonance frequency of 400 MHz for protons. The self-diffusion coefficients of BTEX molecules, water, and RL micelles were measured by the pulsed magnetic field gradient method using a stimulated spin echo pulse sequence.<sup>[62]</sup> The amplitude of the stimulated spin echo signal is given by

$$A(\tau, \tau_1, g, \delta) \propto \exp\left(-\frac{2\tau}{T_2} - \frac{\tau_1}{T_1}\right) \exp(-\gamma^2 \delta^2 g^2 D t_d), \quad (1)$$

where  $T_1$  and  $T_2$  are spin-lattice and spin-spin NMR relaxation times, respectively;  $\tau$  and  $\tau_1$  are time intervals;  $\gamma$  is the gyromagnetic ratio for protons;  $g$  and  $\delta$  are amplitude and duration of the pulse field gradient pulses, respectively;  $D$  is the diffusion coefficient; and  $t_d = (\Delta - \delta/3)$  is the diffusion time,  $\Delta = (\tau + \tau_1)$ .

In the measurements, the magnitude of the impulse gradient was varied,  $g_{\max} = 2\text{--}4\text{ T/m}$ ; the other parameters were not changed and amounted to  $\tau_d = 50\text{ ms}$ , number of scans  $NS = 4$ . The preliminarily measured

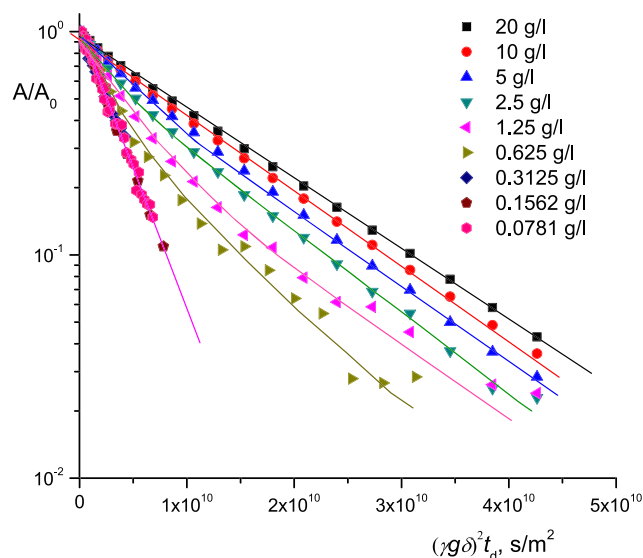


**FIGURE 3** Diffusion decays of  $^1\text{H}$  nuclear magnetic resonance (NMR) spectrum lines of methylene protons of rhamnolipids in  $\text{D}_2\text{O}$  solutions at concentrations of the RLs from 20 to 0.0781 g/L.  $T = 298\text{ K}$ .

time of spin-lattice relaxation of oxyethylene protons of RL was  $\approx 0.5\text{ s}$ ; in accordance with this, the time between successive scans was set to  $RT = 5\text{ s}$ . Diffusion decays were processed, and diffusion coefficients were determined using Bruker TopSpin 3.5 software. The coefficients of self-diffusion of RLs were determined from the decays of the integral intensities of the proton lines of the methylene groups. The  $^1\text{H}$  NMR spectrum of RLs in a saturated solution of benzene is shown in Figure 2. As can be seen from Figure 2, the spectral lines of aromatic protons of benzene (as well as other representatives of BTEX) do not overlap with the spectral lines of the methylene groups of RLs, which greatly simplifies the processing of diffusion decays.

Diffusion decays are dependences of  $\ln(A)$  on  $\gamma^2 \delta^2 g^2 t_d$ . Diffusion decays obtained for RLs at high concentrations in water in the absence of (0.6–20 g/L) and in the presence of BTEX (0.6–200 g/L) were non-single linear in form (Figure 3). At the same time, the diffusion decays of other components (water and BTEX) in all solutions at all concentrations of RLs were linear. The nonlinearity of diffusion declines in RLs can be explained by their complex fractional composition, which is a mixture of mono- and di-RLs with variations in the length and degree of branching of fatty acid chains.<sup>[75–77]</sup> Due to different translational mobility and different values of  $D$  of different fractions, the resulting diffusion decay of the echo signal becomes nonlinear. The presence of RL monomers and micelles in solution can also lead to nonlinear

diffusion decays in the case of a slow (on the NMR scale) exchange of molecules between the micellar and monomeric forms.<sup>[78,79]</sup> Processing of nonlinear diffusion decays for RLs was performed in two ways: (a) by the initial parts of the decays and (b) by decomposition into two exponentials.

The slopes of the initial parts of the diffusion decays can be used to determine the effective diffusion coefficients of RLs, assuming that the initial parts of the decays contain information about all fractions and aggregates.<sup>[80]</sup> Decomposition of the nonlinear decay into a sum of two or more exponential ones makes it possible to determine the diffusion coefficients and the relative fractions of individual forms (monomers, micelles and other aggregates, aggregates). For reliable decomposition, it is necessary that the dynamic range of the decay of the spin echo signal be at least one order of magnitude, and diffusion coefficients of individual forms must differ significantly from each other:

$$A(\tau, \tau_1, g, \delta) \propto A_0 \sum P_i \exp\left(-\frac{2\tau}{T_{2i}} - \frac{\tau_1}{T_{1i}}\right) \exp(-\gamma^2 \delta^2 g^2 D_i t_d), \quad (2)$$

where  $P_i$  and  $D_i$  are the fraction and the diffusion coefficient of the  $i$ th fraction, respectively.

### 2.3 | Dynamic light scattering

The sizes of micelles and aggregates in aqueous H<sub>2</sub>O solutions of RLs were also measured by DLS using a Zetasizer Nano-ZS (Malvern Instruments, Ltd., Malvern, U.K.). An He–Ne laser with  $\lambda = 632.8$  nm was used.<sup>[81]</sup> The dynamic light scattering (also known as PCS—photon correlation spectroscopy) method<sup>[82]</sup> is based on the measurement of temporal fluctuations of light scattered by particles (micelles, aggregates) with sizes of 0.6 nm to 6  $\mu$ m performing Brownian motion in a micellar solution. The relationship between the size of a particle and its velocity due to Brownian motion is defined in the Stokes–Einstein equation. The measurements were performed in disposable sizing cuvettes. The samples were equilibrated for 5 min prior to measurement. Thereafter, three consecutive measurements were performed at a 1-min interval to ensure that the system had reached the steady state. The DLS data were analyzed by the cumulant method. The particle diameter values obtained from the size distribution by volume presented in the results are the average of three replicates. Before measurements were taken, RL solutions obtained by successive dilutions were kept for 2 days.

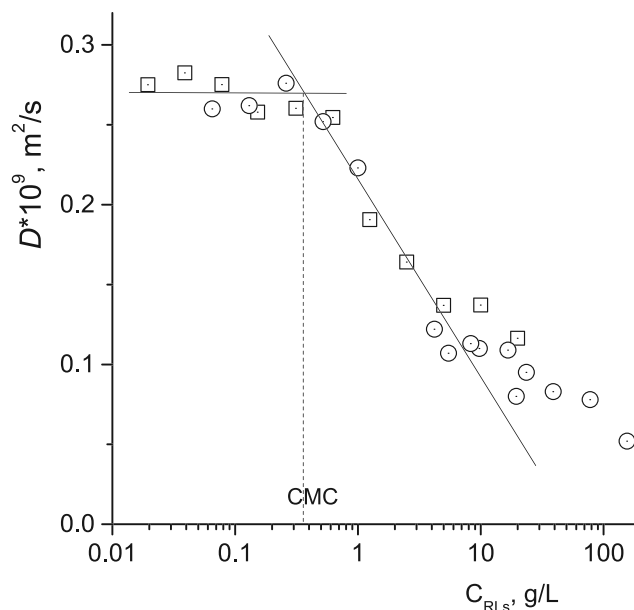


**FIGURE 4** Coefficients of diffusion of rhamnolipid molecules depending on the concentration of rhamnolipid in an aqueous D<sub>2</sub>O solution at 298 K. (The results of two independent series are presented as circle and square symbols.)

### 2.4 | Conductometry

The concentration dependence of the specific electrical conductivity of surfactant solutions at  $C = \text{CMC}$  has a characteristic kink<sup>[83,84]</sup> due to an increase in particle size upon transition from the molecular to micellar state. In measurements of the electrical conductivity of RL solutions, a cell with a two-point arrangement of electrodes was used; the measuring cell was calibrated using standard solutions of potassium chloride. To eliminate the effects of polarization of electrodes, we used an RLC APPA 701 AC conductometer with operating frequencies from 100 Hz to 100 kHz.

## 3 | RESULTS AND DISCUSSION

### 3.1 | CMC of RLs in aqueous solutions

Methods for determining the CMC of surfactants are based on characteristic changes (kinks) in the surface or bulk properties of surfactant solutions during the transition from the monomeric, molecular state of surfactants to the aggregated, micellar state. The formation of micelles is preceded by the region of the pre-micellar state.<sup>[85,86]</sup> The determination of the CMC of RLs in aqueous solutions is mainly carried out by changing the surface tension coefficient,<sup>[5,24,25,77]</sup> measured by changes in density, viscosity, or electrical conductivity<sup>[26]</sup> and



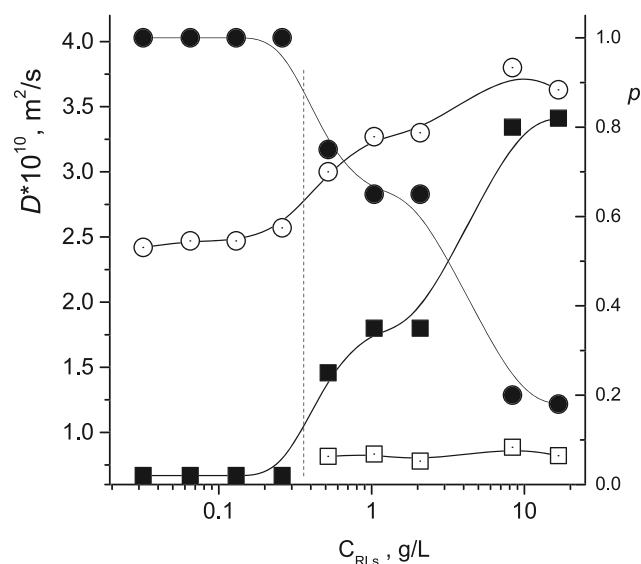


**FIGURE 5** Diffusion coefficients (open symbols) and relative fractions (closed symbols) of monomers (circle) and micelles (square) in aqueous D<sub>2</sub>O solutions.  $T = 25^{\circ}\text{C}$ .

calculated theoretically.<sup>[23]</sup> Micellization in surfactant solutions is also studied using NMR by analyzing changes in the characteristics of spectral lines, the magnitude of the chemical shift and the width and shape of the line, and the dependences of diffusion coefficients of surfactant molecules on concentration, temperature, the presence of co-surfactants, and other components of the solution.<sup>[66,67,72]</sup> We have measured the CMC of RLs in aqueous solutions by NMR diffusometry, dynamic light scattering, and conductometry.

The result of a decrease in the mobility of RL molecules during the transition from the monomeric to micellar state is a sharp decrease in the effective diffusion coefficient, which is determined from the initial section of the diffusion decay, Figure 4. The break point of the dependence of the effective diffusivity on the concentration of RL in solution, corresponding to  $C = \text{CMC}$ , is observed at  $C \approx 0.35 \text{ g/L}$ .

Figure 5 shows the results of decomposition of diffusion decays into two exponential components corresponding to the monomeric and micellar state of RLs in solutions. The decomposition procedure was performed using the spectrometer software TopSpin.<sup>[87]</sup> At  $C_{\text{RLS}} < 0.35 \text{ g/L}$ , the decays are single exponential, which corresponds to the monomeric state of RLs. At  $C_{\text{RLS}} > 0.35 \text{ g/L}$ , the decays become non-exponential, and they are well-described by two exponents corresponding to the monomeric and micellar states. At  $C_{\text{RLS}} > 0.35 \text{ g/L}$ , the relative fraction of micelles increases, and the relative fraction of monomers decreases with increasing RL

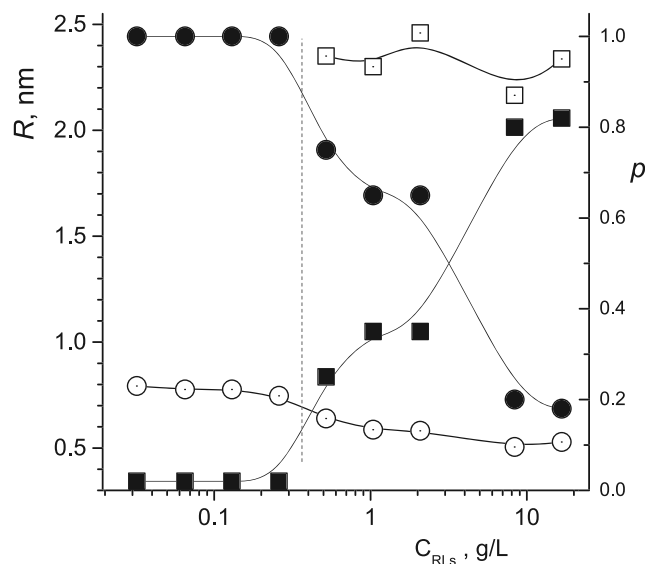


**FIGURE 6** Effective hydrodynamic radii (open symbols) and fractions (closed symbols) of monomers (circle) and micelles (square) in aqueous D<sub>2</sub>O solutions according to the results of NMR diffusometry.  $T = 25^{\circ}\text{C}$ .

concentration. The transition from the monomeric to micellar state apparently occurs at  $C \approx 0.35 \text{ g/L}$ .

The transition from the monomeric, molecular state of RLs in solution to the micellar, aggregated state can be detected by the change in the size of the kinetic units (monomers or micelles) formed by RLs. The so-called effective hydrodynamic radii of particles can be obtained from the results of NMR diffusometry and using the method of dynamic light scattering. Both methods use the hydrodynamic Stokes–Einstein relation to calculate particle sizes<sup>[73]</sup>:

$$R = \frac{kT}{6\pi\eta D}, \quad (3)$$

where  $k$  is the Boltzmann constant and  $\eta$  is the dynamic viscosity of the solvent. The calculations are carried out in the approximation of the spherical shape of the diffusing particles; accordingly, the resulting radius is the effective hydrodynamic radius.

NMR diffusometry makes it possible to determine the effective sizes of both monomers and micelles. The dynamic light scattering method is insensitive to monomers but provides information about aggregates with sizes much larger than those of micelles. The latter task is problematic for the NMR method, due to errors in the decomposition of the diffusion decay into the sum of exponentials, small diffusion components of the aggregates, and their low fractions. It can be argued that the

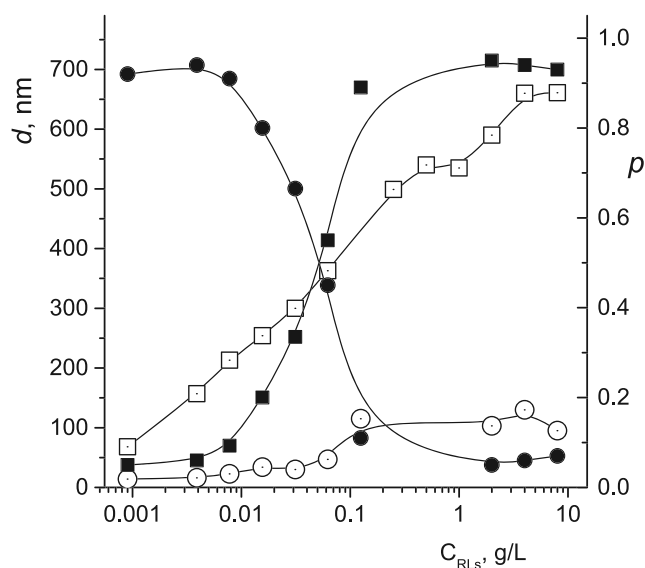


**FIGURE 7** Hydrodynamic diameters (open symbols) and fractions (closed symbols) of micelles (circle) and aggregates (square) in aqueous  $D_2O$  solutions according to the results of DLS measurements.  $T = 25^\circ C$ .

methods of NMR diffusometry and dynamic light scattering complement each other.

Based on the values of diffusion coefficients of monomers and aggregates obtained by NMR diffusometry, by decomposition, the diffusion decays into a sum of two exponentials. Using relation (3), we calculate the effective hydrodynamic radii of monomers and aggregate RLs in solution. The value of the coefficient of dynamic viscosity of heavy water at 298 K is taken as equal to 1.138 mPa s.<sup>[88]</sup> The results are presented in Figure 6.

According to the results of NMR diffusometry, the effective hydrodynamic radii of monomer RLs are 0.7–0.8 nm; calculations by the atomic increment method<sup>[73,89]</sup> give a value of  $\approx 0.53$  nm. The effective hydrodynamic radii of RL micelles are in the range of 2.1–2.4 nm. The CMC value is easily determined by the characteristic breaks on all curves and is approximately 0.35 g/L.

According to the results of DLS measurements in Figure 7, aggregation of RLs molecules in aqueous  $H_2O$  solutions is already detected at relatively low concentrations  $C \approx 0.001$  g/L. In the entire range of concentrations, RL molecules form both micelles and aggregates, the sizes of which significantly exceed the sizes of micelles. Effective hydrodynamic diameters of micelles at  $C \leq 0.05$  g/L average 20 nm and at  $C \geq 0.05$  g/L average about 100 nm. The effective hydrodynamic diameters of aggregates increase monotonically from 70 nm at  $C = 0.001$  g/L to 700 nm at  $C = 8$  g/L. With an increase in the concentration of RLs, changes in the relative

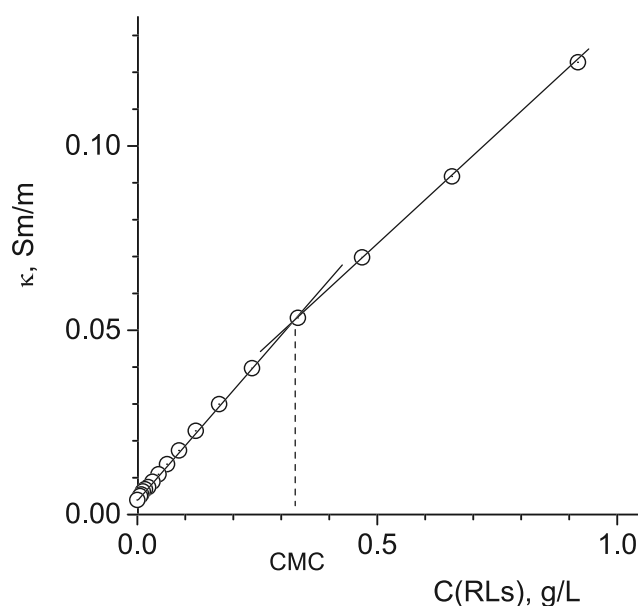


**FIGURE 8** Electrical conductivity of aqueous ( $H_2O$ ) solutions of rhamnolipids.  $T = 298$  K.

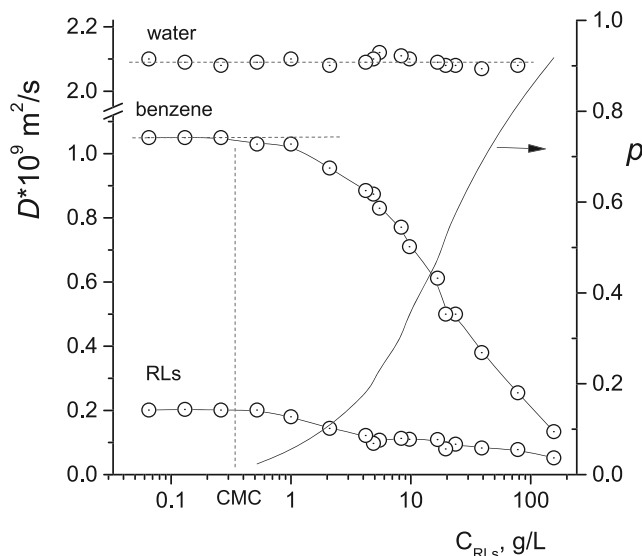


**FIGURE 9** Diffusion coefficients of rhamnolipid, benzene, and water in aqueous  $D_2O$  solutions depending on the concentration of RLs in the solution and fraction of solubilized benzene molecules.  $T = 298$  K.

proportions of micelles and aggregates are observed; at low concentrations, micelles predominate, and at high concentrations, aggregates predominate. The concentration range of 0.01–0.1 g/L corresponds to the transition from one supramolecular structural form to another, from micelles to aggregates.

We can note the qualitative agreement between the results of estimating the sizes of micelles obtained by NMR diffusometry and DLS. According to NMR

diffusometry, the formation of micelles and an increase in their shape at  $C \approx 0.1\text{--}0.3$  g/L are observed. According to DLS data, the formation of large aggregates is observed in the same region, and their fraction increases with the concentration of RLs in solution. The results of DLS measurements are shown in Figure 9.

Figure 8 shows the results of measurements of the electrical conductivity of aqueous solutions of RLs in ordinary ( $\text{H}_2\text{O}$ ) water at 298 K, performed at a frequency of 100 Hz. The inflection point of the dependence of the electrical conductivity on the concentration of RLs in the solution, corresponding to the critical micelle concentration, is observed at  $C = 0.33$  g/L.

The results of measurements of CMC RLs by NMR diffusometry, dynamic light scattering, and electrical conductivity are in good agreement with each other, with the average CMC value at 298 K being  $\sim 0.34$  g/L. In their work,<sup>[90]</sup> da Silva et al. draw attention to a significant spread in the CMC values of mono-, di-RLs and their mixtures obtained from different samples and by different methods at concentrations from 1 to 400 mg/L. For example, in the works of other authors, CMC values are indicated for RLs: 0.4–0.45 mM,<sup>[24]</sup> 71.5 mg/L,<sup>[25]</sup>  $\sim 80$   $\mu\text{M}$ ,<sup>[31]</sup> 150  $\mu\text{M}$ ,<sup>[32]</sup> 45 mg/L.<sup>[33]</sup>

### 3.2 | Solubilizing properties of micellar solutions of RLs

The NMR diffusometry method is effectively used to study solubilization processes, that is, the processes of introducing substances insoluble or poorly soluble in water into micelles, leading to an increase in their conditional solubility and use for their extraction.<sup>[91]</sup> We used this method to study the solubilizing properties of RLs in aqueous solutions. Substances of the BTEX group (benzene, toluene, ethylbenzene, and xylene) were used as solubilizates. The initial concentrations of BTEX corresponded to their limiting solubilities, and all measurements were performed at 298 K.

By measuring diffusivities of all components in an aqueous solution of surfactant + solubilizate, one can answer the question of how the solubilizate is distributed between the bound (as part of micelles) and free (in water) states. In such a two-phase model, the diffusivity of the solubilizate molecules in solution is represented as<sup>[70,91]</sup>

$$D_S = p \cdot D_S^{\text{mic}} + (1 - p) \cdot D_S^{\text{free}}, \quad (4)$$

where  $p$  is the fraction of the solubilizate molecules in micelles and  $D_S^{\text{mic}}$  and  $D_S^{\text{free}}$  are diffusivities of molecules

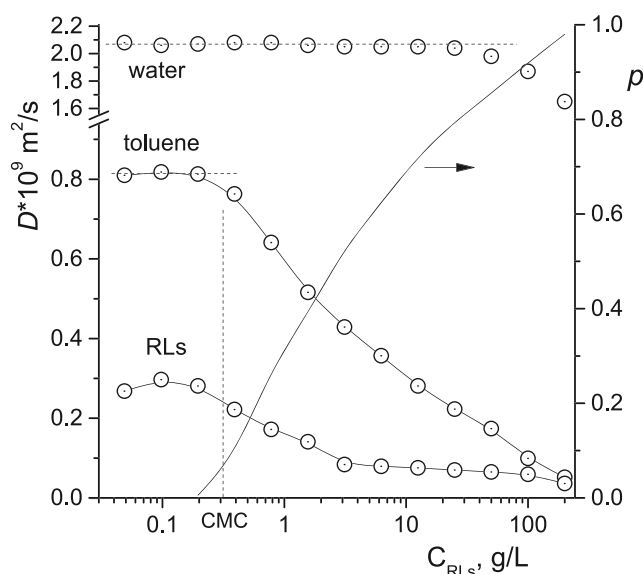


**FIGURE 10** Diffusion coefficients of rhamnolipid, toluene, and water in aqueous  $\text{D}_2\text{O}$  solutions depending on the concentration of rhamnolipid and the fraction of solubilized molecules of toluene.  $T = 298$  K.

of solubilizate in micelles and in free state in the solution. Therefore,

$$p = \frac{D_S^{\text{free}} - D_S}{D_S^{\text{free}} - D_S^{\text{mic}}}. \quad (5)$$

At  $C_{\text{surf}} > \text{CMC}$ , diffusion coefficient  $D_S^{\text{mic}}$  can be taken as the measured  $D$  of the surfactant. Accordingly,  $D_S^{\text{free}}$  can be set equal to the  $D$  of the solubilizate in solution, measured in the absence of a surfactant or with a surfactant  $C_{\text{surf}} < \text{CMC}$ .

Figure 9 shows the results of measurements of the diffusion coefficients of individual components in an aqueous  $\text{D}_2\text{O}$  solution of RLs with benzene depending on the concentration of the RL. In the absence of micelles at  $C < \text{CMC}$ , the self-diffusion coefficients of benzene molecules and RLs remain constant. At  $C > \text{CMC}$ , micelles are formed, which leads to a decrease in the diffusion coefficient of RL. Simultaneously with the formation of micelles, the SDC of benzene decreases, which indicates the solubilization of benzene molecules by micelles. As the concentration of RLs increases,  $D$  of benzene approaches that of micelles, indicating a high degree of solubilization of benzene by micelles. The proportion of benzene molecules solubilized by micelles increases from zero at  $C \leq \text{CMC}$  to 0.92 at a concentration of RL  $C = 160$  g/L.

Similar measurements of the diffusivities of individual components were carried out in aqueous  $\text{D}_2\text{O}$



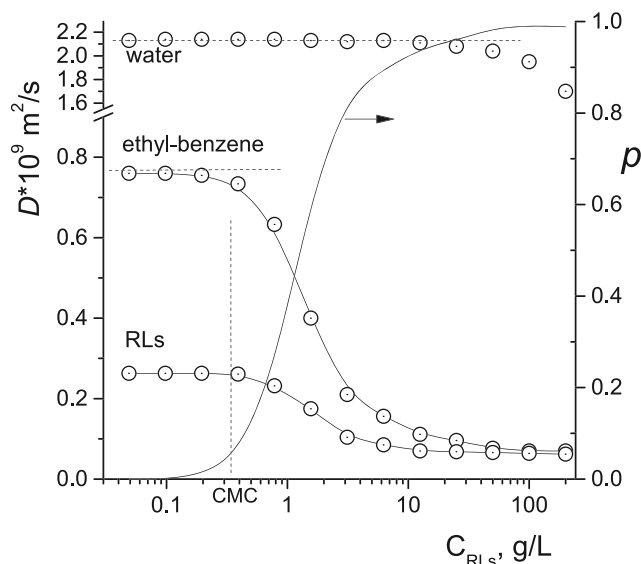


**FIGURE 11** Diffusion coefficients of rhamnolipid, ethylbenzene, and water in aqueous D<sub>2</sub>O solutions depending on the concentration of rhamnolipid in solution and fraction of solubilized molecules of ethylbenzene.  $T = 298$  K.

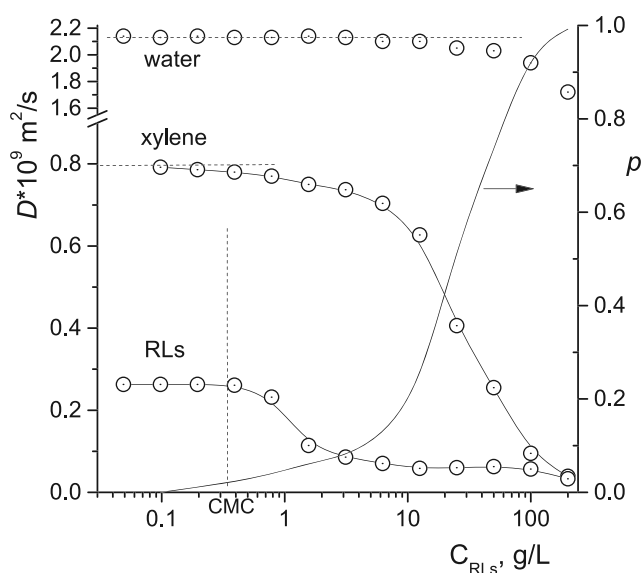


**FIGURE 12** Diffusion coefficients of rhamnolipid, para-xylene, and water in aqueous D<sub>2</sub>O solutions depending on the concentration of rhamnolipid in the solution and the fraction of solubilized molecules of para-xylene.  $T = 298$  K.

solutions of RLs in the presence of other representatives of BTEX: toluene, para-xylene, and ethylbenzene. The results of measurements and the results of calculations of the fraction of solubilized molecules are shown in Figures 10–12.

As can be seen from Figures 9–12, diffusion coefficients of BTEX molecules in all solutions at  $C < \text{CMC}$  are

equal to the  $D$ s of the corresponding BTEX measured in BTEX solutions in D<sub>2</sub>O in the absence of RLs. At  $C > \text{CMC}$ , with an increase in the concentration of RLs in solutions,  $D$ s of BTEX sharply, by almost an order of magnitude, decrease and become equal to the  $D$ s of RLs at high concentrations. Therefore, in all solutions at  $C > \text{CMC}$ , solubilization of BTEX by RLs micelles is observed, whereas at  $C < \text{CMC}$ , solubilization is not observed. At the same time, water molecules are bound by micelles to a much lesser extent;  $D$ s values of water molecules remain constant and do not depend on the presence and concentration of RLs in solution. Only at high concentrations of RLs, due to an increase in hydrodynamic interactions with micelles, a slight decrease (within 10–20%) of the diffusivity of water is observed. At high concentrations of RLs, about 200 g/L, the fraction of solubilized BTEX molecules is close to 100%; almost all BTEX molecules are in a solubilized state in RL micelles.

The solubilization characteristics of RLs with respect to substances of the BTEX group are summarized in Table 1, where, in addition to the fraction of solubilized molecules  $p$ , the micelle-water partition coefficient  $K_m$  and molar solubilization ratio  $MSR$  are also indicated. The micelle-water partition coefficient  $K_m$  is equal to the ratio of the number of moles of solubilize in micelles to the number of moles of solubilize in the aqueous phase:

$$K_m = \frac{p}{1-p}. \quad (6)$$

The molar solubilization ratio  $MSR$  is equal to the ratio of the molar concentration of solubilized molecules  $C_{sol}^{mic}$  to the molar concentration of surfactants in the micellar state  $C_{surf}^{mic}$ :

$$MSR = \frac{C_{sol}^{mic}}{C_{surf}^{mic}} = \frac{p \cdot C_{sol}^{total}}{C_{surf}^{total} - \text{CMC}}, \quad (7)$$

where  $C_{sol}^{total}$  and  $C_{surf}^{total}$  are total molar concentrations of solubilize and surfactant in solution.

Our results can be compared with the results of previous works<sup>[38–40]</sup> devoted to studies of the solubilization of aromatic hydrocarbons using RLs. The results<sup>[38,39]</sup> showed that the solubilities of naphthalene, phenanthrene, and pyrene increased linearly with the rise of the RL biosurfactant dose above the biosurfactant critical micelle concentration. It has been established that the effectiveness of solubilization is influenced by factors such as biosurfactant concentration, pH, ionic strength, and temperature. Using spectrophotometry, investigation

TABLE 1 Solubilization characteristics of rhamnolipids.

$C_{RLs}$ , g/L	Benzene			Toluene			Ethylbenzene			Xylene		
	$p$	$K_m$	$MSR$	$p$	$K_m$	$MSR$	$p$	$K_m$	$MSR$	$p$	$K_m$	$MSR$
0.5	0.02	0.02	0.70	0.16	0.19	4.48	0.13	0.15	0.80	0.03	0.02	0.20
1	0.05	0.05	0.40	0.3	0.43	1.63	0.37	0.59	0.53	0.05	0.05	0.08
5	0.21	0.27	0.24	0.58	1.38	0.44	0.87	6.69	0.17	0.11	0.12	0.024
10	0.36	0.56	0.20	0.69	2.22	0.25	0.92	11.5	0.09	0.2	0.25	0.02
20	0.65	1.86	0.17	0.77	3.35	0.14	0.95	19	0.04	0.42	0.72	0.02
50	0.73	2.70	0.08	0.85	5.67	0.06	0.98	49	0.02	0.73	4.30	0.015
100	0.85	5.67	0.05	0.92	11.5	0.03	0.99	99	0.01	0.92	11.5	0.01

of solubilization of PAHs (Nap, Phe, and Py) by single and binary mixed RL–sophorolipid biosurfactants gives  $MSR$  values in the range of 0.01–1.<sup>[40]</sup>

For instance, the results<sup>[35]</sup> show that the apparent solubility of the four alkanes (decane, dodecane, tetradecane, and hexadecane) increases linearly with the increase of di-RL concentration at di-RL concentrations below CMC. The solubilization potential of di-RL indicated by the molar solubilization ratio ( $MSR$ ) is higher at sub-CMC than at hyper-CMC concentrations, with the  $MSR$  for n-dodecane equal to 2.91,<sup>[46]</sup> and for n-hexadecane equal to 5.2.<sup>[37]</sup>

## 4 | CONCLUSIONS

We studied the micellar and solubilizing properties of unfractionated RL in aqueous solutions at a temperature of 298 K at RL concentrations from 0.0195 to 156 g/L. The compounds of the BTEX group (benzene, toluene, ethylbenzene, and xylene) were studied as solubilizates, where the initial concentrations corresponded to their limiting solubilities in water. Volatile aromatic hydrocarbons, degradation and refining products of oil are soil, air and water pollutants. Removing BTEX from the environment is an urgent task. The use of biological surfactants, including RLs, for the purpose of micellar extraction of pollutants is dictated by their low toxicity and high biodegradability compared to synthetic surfactants.

The CMC values of the RLs used in this work were determined at 298 K by NMR diffusometry, dynamic light scattering, and conductometry. Within the error limits of the measurement methods,  $CMC \approx 0.35$  g/L. Taking into account the spread of CMC values for mono-, di-rhamnolipids and their mixtures, the value obtained here is in good agreement with the literature data. Based on the results of NMR diffusometry using the Stokes–Einstein relation, the effective hydrodynamic radii of molecules and micelles RLs were calculated, and the

relative content of micelles and aggregates in solution was estimated. The conclusions of NMR diffusometry agree qualitatively with the results of DLS. According to NMR diffusometry and DLS data, micelles form in the concentration range  $C \approx 0.1$ – $0.3$  g/L. According to DLS data, the formation of large aggregates is observed in the same region, the fraction of which increases with an increase in the concentration of RLs in the solution.

The solubilizing properties of micellar solutions of RLs with respect to BTEX compounds were studied by NMR diffusometry, which makes it possible to selectively measure diffusivities of molecules of individual components in solution—water, solubilizate, and RLs. Different or close values of diffusivities of BTEX molecules and RLs micelles allow us to draw conclusions about the occurrence of solubilization and its effectiveness. The formation of micelles at  $C > CMC$  is reflected in a decrease in  $D$  of RL, simultaneously with the formation of micelles.  $D$  of the solubilizate decreases, which indicates solubilization of its molecules by micelles. In all solutions, solubilization of BTEX compounds is observed, starting from the concentration of RLs  $\geq CMC$ . With an increase in the concentration of RLs up to  $\sim 100$ – $200$  g/L, the solubilizate is completely contained in the micelles. The distribution coefficient of the solubilizate between the aqueous and micellar phases was determined based on the results of selective measurements of diffusivities in solutions of RLs in  $D_2O$  water in the presence of substances of the BTEX group.

## ACKNOWLEDGMENTS


We thank Scriptia Academic Editing for the English correction and proofreading of this manuscript. V.P.A., R.V.A., and E.V.P. acknowledge the Ministry of Science and Higher education of the Russian Federation and Program Priority-2030 for Kazan Federal University for their support. The DLS study was carried out using the equipment of the Center for Collective Use “Nanomaterials and Nanotechnology” of the Kazan National Research

Technological University with the financial support of the Ministry of Science and Higher Education of the Russian Federation under agreement No. 075-15-2021-699.

## PEER REVIEW

The peer review history for this article is available at <https://publons.com/publon/10.1002/mrc.5337>.

## ORCID

Victor P. Arkhipov  <https://orcid.org/0000-0003-4131-9934>

Ekaterina V. Petrova  <https://orcid.org/0000-0002-4273-3443>

Andrei Filippov  <https://orcid.org/0000-0002-6810-1882>

## REFERENCES

- [1] D. S. Pardhi, R. Bhatt, R. R. Panchal, V. H. Raval, K. N. Rajput, in *Microbial Surfactants*, CRC Press, Boca Raton **2021**, 27.
- [2] A. Devale, R. Sawant, K. Pardesi, S. Satpute, S. Mujumdar, in *Microbial Surfactants*, CRC Press, Boca Raton **2022**, 208.
- [3] S. Vijayakumar, V. Saravanan, *Res. J. Microbiol.* **2015**, *10*, 181.
- [4] A. M. Abdel-Mawgoud, F. Lépine, E. Déziel, *Appl. Microbiol. Biotechnol.* **2010**, *86*, 1323.
- [5] P. Kopalle, S. A. Pothana, S. Maddila, *Chem. Data Collect.* **2022**, *41*, 100905.
- [6] A. N. Mendes, L. A. Filgueiras, J. C. Pinto, M. Nele, *J. Biomater. Nanobiotechnol.* **2015**, *6*, 64.
- [7] H. Abbasi, F. J. Aranda, K. A. Noghabi, A. Ortiz, *Biochim. Biophys. Acta, Biomembr.* **2013**, 1828, 2083.
- [8] T. T. Nguyen, N. H. Youssef, M. J. McInerney, D. A. Sabatini, *Water Res.* **2008**, *42*, 1735.
- [9] G. Liu, H. Zhong, X. Yang, Y. Liu, B. Shao, Z. Liu, *Biotechnol. Bioeng.* **2018**, *115*, 796.
- [10] C. N. Mulligan, S. Wang, *Engin. Geol.* **2006**, *85*, 75.
- [11] K. Urum, T. Pekdemir, *Chemosphere* **2004**, *57*, 1139.
- [12] Z. Zeng, Y. Liu, H. Zhong, R. Xiao, G. Zeng, Z. Liu, L. Qin, *Sci. Total Environ.* **2018**, *634*, 1.
- [13] L. Magalhães, M. Nitschke, *Food Control* **2013**, *29*, 138.
- [14] N. Lourith, M. Kanlayavattanukul, *Int. J. Cosmetic Sci.* **2009**, *31*, 255.
- [15] X. Vecino, J. M. Cruz, A. B. Moldes, L. R. Rodrigues, *Crit. Rev. Biotechnol.* **2017**, *37*, 911.
- [16] Z. A. A. Aziz, S. H. M. Setapar, A. Khatoon, A. Ahmad, in *Current Trends and Future Prospects* (Eds: H. Sarma, M. Narasimha, V. Prasad), J. Wiley & Sons, Chichester **2021**, 397.
- [17] S. G. Costa, M. Nitschke, F. Lépine, E. Déziel, J. Contiero, *Process Biochem.* **2010**, *45*, 1511.
- [18] X. Long, G. Zhang, C. Shen, G. Sun, R. Wang, L. Yin, Q. Meng, *Bioresour. Technol.* **2013**, *131*, 1.
- [19] B. E. Igiri, S. I. Okoduwa, G. O. Idoko, E. P. Akabuogu, A. O. Adeyi, I. K. Ejiogu, *J. Toxicol.* **2018**, *2018*, 2568038.
- [20] J. Tang, J. He, X. Xin, H. Hu, T. Liu, *Chem. Eng. J.* **2018**, *334*, 2579.
- [21] W. Chen, Y. Qu, Z. Xu, F. He, Z. Chen, S. Huang, Y. Li, *Environ. Sci. Pollut. Res.* **2017**, *24*, 16344.
- [22] M. Irfan-Maqsood, M. Seddiq-Shams, *Indust. Biotechnol.* **2014**, *10*, 285.
- [23] I. E. Kłosowska-Chomiczewska, K. Mędrzycka, E. Hallmann, E. Karpenko, T. Pokynbroda, A. Macierzanka, C. Jungnickel, *J. Coll. Interf. Sci.* **2017**, *488*, 10.
- [24] L. M. Wu, L. Lai, Q. Lu, P. Mei, Y. Q. Wang, L. Cheng, Y. Liu, *Coll. Surf. B: Biointerfaces* **2019**, *181*, 593.
- [25] M. Sánchez, F. J. Aranda, M. J. Espuny, A. Marqués, J. A. Teruel, Á. Manresa, A. Ortiz, *J. Coll. Interf. Sci.* **2007**, *307*, 246.
- [26] D. Mańko, A. Zdziennicka, B. Jańczuk, *Coll. Surf. B: Biointerfaces* **2014**, *119*, 22.
- [27] D. Kitamoto, T. Morita, T. Fukuoka, M. A. Konishi, T. Imura, *Curr. Opinion Coll. Interf. Sci.* **2009**, *14*, 315.
- [28] M. L. Chen, J. Penfold, R. K. Thomas, T. J. P. Smyth, A. Perfumo, R. Marchant, I. Grillo, *Langmuir* **2010**, *26*, 18281.
- [29] O. Pornsunthorntawe, S. Chavadej, R. Rujiravanit, *Coll. Surf. B: Biointerfaces* **2009**, *72*, 6.
- [30] J. T. Champion, J. C. Gilkey, H. Lamparski, J. Retterer, R. M. Miller, *J. Coll. Interface Sci.* **1995**, *170*, 569.
- [31] H. Zhong, L. Yang, X. Yang, G. Zeng, Z. Liu, Y. Liu, X. Yuan, *RSC Adv.* **2015**, *5*, 88578.
- [32] Ş. Ş. Helvacı, S. Peker, G. Özdemir, *Coll. Surf. B: Biointerfaces* **2004**, *35*, 225.
- [33] Z. A. Raza, Z. M. Khalid, M. S. Khan, I. M. Banat, A. Rehman, A. Naeem, M. T. Saddique, *Biotechnol. Lett.* **2010**, *32*, 811.
- [34] Y. Guo, C. N. Mulligan, M. P. Nieh, *Coll. Surf. A: Physicochem. Engin. Asp.* **2011**, *373*, 42.
- [35] X. Yang, F. Tan, H. Zhong, G. Liu, Z. Ahmad, Q. Liang, *Coll. Surf. B: Biointerfaces* **2020**, *192*, 111049.
- [36] I. E. Kłosowska-Chomiczewska, A. Kotewicz-Siudowska, W. Artichowicz, A. Macierzanka, A. Głowacz-Różyńska, P. Szumala, C. Jungnickel, *Molecules* **2021**, *26*, 26.
- [37] Y. Zhang, R. M. Miller, *Appl. Environ. Microbiol.* **1995**, *61*, 2247.
- [38] S. Li, Y. Pi, M. Bao, C. Zhang, D. Zhao, Y. Li, J. Lu, *Marine Pollut. Bull.* **2015**, *101*, 219.
- [39] H. Yu, G. Huang, J. Wei, C. An, *J. Environ. Quality* **2011**, *40*, 477.
- [40] D. Song, S. Liang, L. Yan, Y. Shang, X. Wang, *J. Environ. Quality* **2016**, *45*, 1405.
- [41] A. Bodagh, H. Khoshdast, H. Sharafi, H. Shahbani Zahiri, K. Akbari Noghabi, *Indust. Engin. Chem. Res.* **2013**, *52*, 3910.
- [42] M. Moreno, L. P. Mazur, S. E. Weschenfelder, R. J. Regis, R. A. de Souza, B. A. Marinho, A. A. U. de Souza, *J. Water Proc. Engin.* **2022**, *46*, 102574.
- [43] E. Abbasi-Garravand, C. N. Mulligan, *Separ. Purif. Technol.* **2014**, *132*, 505.
- [44] C. Munoz-Cupa, A. Bassi, L. Liu, *Canadian J. Chem. Engin.* **2022**, *100*, 2322.
- [45] S. P. Verma, B. Sarkar, *J. Environ. Manage.* **2018**, *213*, 217.
- [46] H. Zhong, X. Yang, F. Tan, M. L. Brusseau, L. Yang, Z. Liu, X. Yuan, *New J. Chem.* **2028**, *2016*, 40.
- [47] H. Abbasi, K. A. Noghabi, M. M. Hamed, H. S. Zahiri, A. A. Moosavi-Movahedi, M. Amanlou, A. Ortiz, *Coll. Surf. B: Biointerfaces* **2013**, *101*, 256.
- [48] O. Fayemiwo, K. Moothi, M. Daramola, *Water Sa* **2017**, *43*, 602.
- [49] I. C. Nisbet, P. K. Lagoy, *Regulatory Toxicol. Pharmacol.* **1992**, *16*, 290.

- [50] World Health Organization. (2017). Guidelines for drinking-water quality: fourth edition incorporating first addendum, 4th ed + 1st add. World Health Organization. <https://apps.who.int/iris/handle/10665/254637>. License: CC BY-NC-SA 3.0 IGO.
- [51] O. Ezquerro, G. Ortiz, B. Pons, M. T. Tena, *J. Chromatogr. A* **2004**, 1035, 17.
- [52] M. A. A. Abadi, M. Masrournia, M. R. Abedi, *Chem. Methodolog.* **2021**, 5, 11.
- [53] J. S. Yadav, C. A. Reddy, *Appl. Environ. Microbiol.* **1993**, 59, 756.
- [54] H. Shim, S. T. Yang, *J. Biotechnol.* **1999**, 67, 99.
- [55] C. E. Flores-Chaparro, M. C. Rodriguez-Hernandez, L. F. Chazaro-Ruiz, M. C. Alfaro-De la Torre, M. A. Huerta-Diaz, J. R. Rangel-Mendez, *J. Water Proc. Engin.* **2021**, 40, 101874.
- [56] S. Nojavan, M. Yazdanpanah, *J. Chromatogr. A* **2017**, 1525, 51.
- [57] M. Zahedniya, Z. G. Tabatabaei, *J. Water Wastewater* **2018**, 29, 1.
- [58] Z. A. M. Hir, R. Ali, *J. Sci. Technol.* **2021**, 4, 25.
- [59] M. Radwan, M. G. Alalm, H. K. El-Etriby, *J. Water Proc. Engin.* **2019**, 31, 100837.
- [60] E. L. Hahn, *Phys. Rev.* **1950**, 80, 580.
- [61] E. O. Stejskal, J. E. Tanner, *J. Chem. Phys.* **1965**, 42, 288.
- [62] J. E. Tanner, *J. Chem. Phys.* **1970**, 52, 2523.
- [63] P. Stilbs, *Progr. Nucl. Magn. Reson. Spectr.* **1987**, 19, 1.
- [64] A. Macchioni, G. Ciancaleoni, C. Zuccaccia, D. Zuccaccia, *Chem. Soc. Rev.* **2008**, 37, 479.
- [65] T. L. James, G. G. McDonald, *J. Magn. Reason.* **1973**, 11, 58.
- [66] O. Söderman, P. Stilbs, W. S. Price, *Concepts Magn. Reason. A* **2004**, 23, 121.
- [67] P. Stilbs, B. Lindman, *J. Phys. Chem.* **1981**, 85, 2587.
- [68] J. Mason (Ed), *Multinuclear NMR*, Springer Science & Business Media, NY **2012**, p. 660.
- [69] P. Stilbs, *Eur. Biophys. J.* **2013**, 42, 25.
- [70] P. Stilbs (Ed), *Diffusion and electrophoretic NMR*, Walter de Gruyter GmbH & Co KG., Berlin. **2019**, p. 332.
- [71] M. J. Thrippleton, N. M. Loening, J. Keeler, *Magn. Reason. Chem.* **2003**, 41, 441.
- [72] W. S. Price, *Diffusion Fundamentals* **2005**, 2, 112.
- [73] J. T. Edward, *J. Chem. Educ.* **1970**, 47, 261.
- [74] H. N. Lekkerkerker, J. K. Dhont, *J. Chem. Phys.* **1984**, 80, 5790.
- [75] M. Nitschke, S. G. Costa, J. Contiero, *Process Biochem.* **2011**, 46, 621.
- [76] A. M. Abdel-Mawgoud, R. Hausmann, F. Lépine, M. M. Müller, E. Déziel (Eds), *Rhamnolipids: detection, analysis, biosynthesis, genetic regulation, and bioengineering of production*, in *Biosurfactants*, Springer, Berlin, Heidelberg **2011** 13.
- [77] E. Haba, A. Pinazo, O. Jauregui, M. J. Espuny, M. R. Infante, A. Manresa, *Biotechnol. Bioeng.* **2003**, 81, 316.
- [78] A. I. Rusanov, *Micellization in surfactant solutions*, Khimija, Moscow **1992**.
- [79] M. Frindi, B. Michels, R. Zana, *J. Phys. Chem.* **1994**, 98, 6607.
- [80] A. I. Maklakov, V. D. Skirda, N. F. Fatkullin, *Self-diffusion in polymer solutions and melts*, Kazan University Press, Kazan **1987**.
- [81] Zetasizer nano series user manual, MAN0317 1 (2004) 2004.
- [82] F. Babick, in *Characterization of nanoparticles*, Elsevier, Amsterdam **2020**, 137.
- [83] W. Al-Soufi, L. Piñeiro, M. Novo, *J. Coll. Interf. Sci.* **2012**, 370, 102.
- [84] M. Pérez-Rodríguez, G. Prieto, C. Rega, L. M. Varela, F. Sarmiento, V. Mosquera, *Langmuir* **1998**, 14, 4422.
- [85] D. N. LeBard, B. G. Levine, R. DeVane, W. Shinoda, M. L. Klein, *Chem. Phys. Lett.* **2012**, 522, 38.
- [86] X. Cui, S. Mao, M. Liu, H. Yuan, Y. Du, *Langmuir* **2008**, 24, 10771.
- [87] <https://www.bruker.com/en/products-and-solutions/mr/nmrsoftware/topspin.html>
- [88] R. C. Hardy, R. L. Cottington, *J. Res. Natl. Bur. Stand.* **1949**, 42, 573.
- [89] A. V. Bondi, *J. Phys. Chem.* **1964**, 68, 441.
- [90] A. R. da Silva, M. Á. Manresa, A. Pinazo, M. T. García, L. Pérez, *Coll. Surf. B: Biointerfaces* **2019**, 181, 234.
- [91] P. Stilbs, *J. Coll. Interf. Sci.* **1983**, 94, 463.

**How to cite this article:** V. P. Arkhipov, R. V. Arkhipov, E. V. Petrova, A. Filippov, *Magn Reson Chem* **2023**, 61(6), 345. <https://doi.org/10.1002/mrc.5337>